Paper no: S30-01

Influence of axial pipe-soil response on pipeline end expansion and walking

by Jean-Christophe Ballard, Filip Van den Abeele, and Charles de Brier
Fugro GeoConsulting, Brussels, Belgium

6th International Pipeline Technology Conference

Thermae Palace Hotel, Ostend, Belgium
6-9 October, 2013

Organized by
Lab. Soete
and Tiratsoo Technical
and supported by
Clarion Technical Conferences
The European Pipeline Research Group

Influence of axial pipe-soil response on pipeline end expansion and walking

DEEPWATER HIGH PRESSURE, high temperature pipelines are generally susceptible to significant end expansion and axial walking. Pipeline walking can cause cumulative axial displacement of the entire pipeline, which can induce damage at termination units, expansion spools and riser tie-ins. The rate of walking depends not only on the temperature profiles, but also on the magnitude of axial resistance, the mobilization distance and the seabed topography.

Assessment of the axial pipe-soil interaction is one of the most critical uncertainties associated with the design of high pressure, high temperature pipelines. In Finite Element (FE) analyses, a simple bi-linear axial response is typically used assuming the same elastic loading-unloading stiffness.

However, Fugro SMARTPIPE measurements have shown a more complex axial response including

1. non-linear first loading behaviour,
2. peak followed by residual resistance,
3. unloading-reloading stiffness higher than the first loading stiffness, and
4. cyclic hardening.

In this paper, parametric FE analyses are presented using the SAGE Profile software suite for offshore pipeline analysis. More sophisticated axial pipe-soil responses, derived from the SMARTPIPE measurements, are implemented to assess the impact on the predicted end expansion and walking rate.

DEEP WATER PIPELINES are left exposed on the seabed and are generally operated under high internal temperature. When pipelines are laid on the seabed and heated, they tend to expand and this expansion is resisted by the axial "friction" mobilised at the pipe-soil interface. Pipeline thermal expansion increases with operating temperature and can become a critical design issue as the capacity of PLETs (PipeLine End Terminations) to absorb expansion has limits (Bruton et al, 2010). When pipelines are cooled during shutdown, they contract but the pipeline ends cannot go back to their original positions because of the axial pipe-soil resistance. During the operational life of the pipeline, the pipeline ends cycle between the heated and cool-down positions.

In some cases, thermal cycling can be accompanied by a global axial movement of the pipeline. This phenomenon is termed pipeline walking. Over a number of start-up and shutdown cycles, walking can lead to significant global displacement of the pipeline and can become a critical design issue. For example, walking can induce damage at termination units, expansion spools and riser tie-ins and may require the pipeline to be stabilised with anchors. A number of mechanisms are known to cause pipeline walking (Carr et al, 2006):

- Seabed slopes along the pipeline length;
- Tension applied to the end of a pipeline by a Steel Catenary Riser (SCR);
- Thermal transients, defined by changes in fluid temperature and thermal loading during shutdown and restart operations;
- Multiphase flow behaviour during shutdown and restart operations.

Axial pipe-soil interaction is one of the most critical uncertainties associated with the design of high pressure, high temperature pipelines and the prediction of end expansion and rate of walking. Considerable capital expenditure can be saved by relatively small adjustment in the magnitude of the expected interaction force. Such saving stems from reduced requirement for stabilisation and anchoring of the pipeline and the reduced need to tolerate end expansion (Hill and Jacob, 2008).

In Finite Element (FE) analyses, a simplistic bi-linear elasto-plastic axial response is typically used for end expansion and walking assessments assuming the same elastic loading-unloading stiffness, as shown in Figure 1. The required input parameters are therefore the limit pipe-soil axial resistance F_{ax} and the associated mobilisation distance D. However, in-situ measurements in deep water soft clay using the Fugro Smartpipe have shown a more complex axial response including:

- Non-linear behaviour;
- Peak resistance followed by a residual resistance;
- Unloading-reloading stiffness higher than the first loading stiffness;
- Cyclic hardening, defined as the progressive increase of axial pipe-soil resistance with operating cycles.

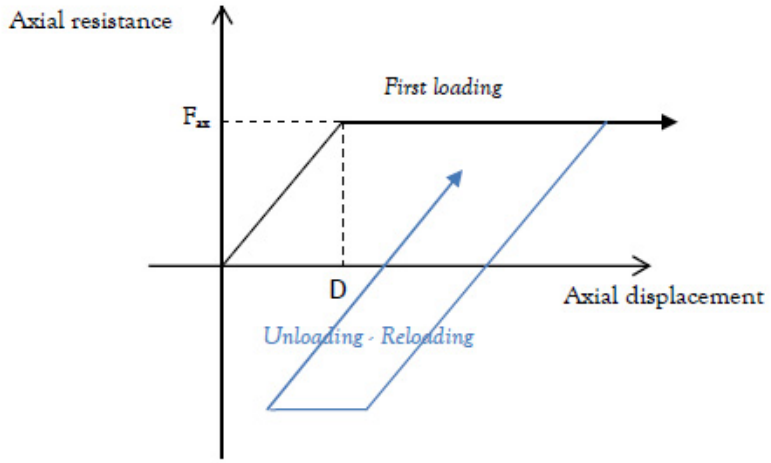

Figure 1 – Typical bi-linear axial response.

In this paper, parametric FE analyses are presented using the SAGE Profile software suite for offshore pipeline analysis. More sophisticated axial pipe-soil responses, derived from typical Smartpipe in-situ measurements, are implemented to assess the impact on the predicted end expansion and walking rate.
Elastic springs are sometimes assumed in FE assessments. This means that the unloading response follows the first loading response and all deformations are recovered. This is of course an erroneous approach as soil deforms plastically. The use of axial soil springs with a plastic memory is instrumental to capture the permanent soil deformation.

Fugro Smartpipe

Fugro Smartpipe is a site investigation tool that is designed to measure pipe-soil interaction forces in-situ, at the seabed, at close to full scale. The equipment comprises a seabed frame with an instrumented model pipe that can be driven in the vertical, axial and lateral directions whilst the corresponding loads and associated excess pore-water pressures are recorded.

A schematic view of Smartpipe is shown in Figure 2. The frame is equipped with various devices including a mini T-bar, a device for measuring settlement of the frame into the seabed, a camera, roll and pitch sensors, etc. The frame is equipped with skirts and mudmats to minimize settlement in soft soil conditions and provide additional stability and reaction during pipe testing.

The current model pipe used with Smartpipe has an outside diameter OD = 225 mm and is 1200 mm long, including dummy sections at each end designed to eliminate end effects. The instrumented central section is mechanically isolated from the end sections and is 776 mm long. The measurement section is equipped with a set of pore-water pressure transducers, as shown on Figure 3. There are five transducers located along the invert of the pipe and four transducers located at 30 degrees from the pipe invert

around the circumference (two on each side). The model pipe is covered with a smooth polypropylene coating. Other model pipes with different diameters and/or coating roughnesses could be used to meet specific project requirements.

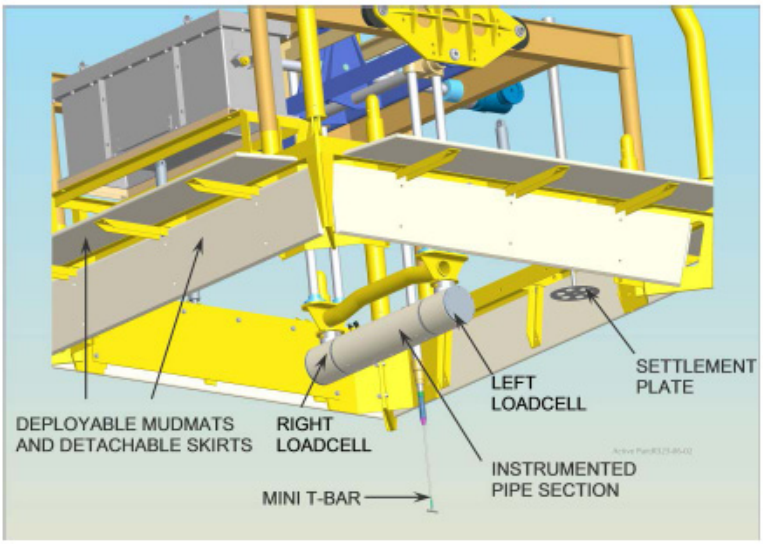

Figure 2 – Schematic view of the Smartpipe.

Load is applied to the pipe by means of a hydraulic system. The pipe can be penetrated vertically under displacement-rate control or load-controlled to a target vertical load or pipe weight. Axial displacement of the pipe at speeds ranging from 0.005 mm/s to 1.15 mm/s, can be applied, covering the typical range that can be experienced by pipelines in the field (Bruton et al, 2008).

More detailed information on Smartpipe can be found in Jacob and Looijen (2008), Hill and Jacob (2008), White et al (2010), Denis and de Brier (2010) and Ballard et al (2013).

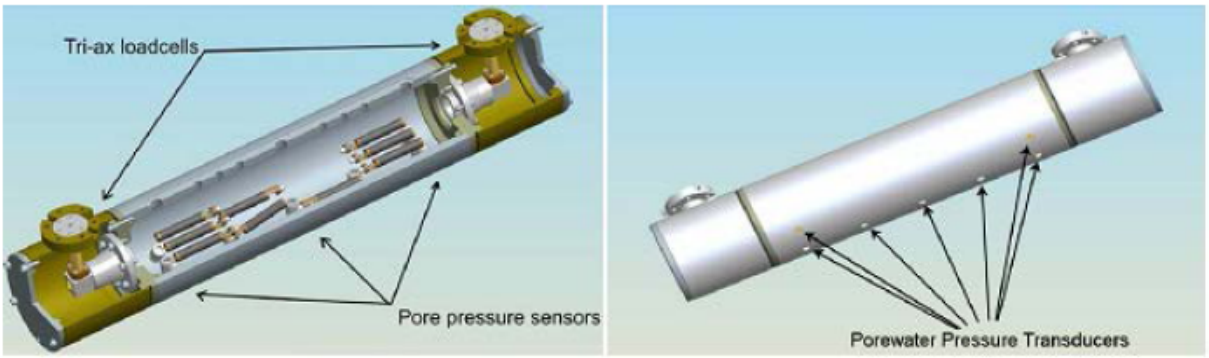

Figure 3 – Cutaway view of model pipe and pore pressure transducers on pipe surface.

Main characteristics of deep water soft clay

The seabed conditions at deep water sites consist mainly of very soft and high plasticity clay, with an undrained shear strength increasing from close to zero at the mudline to about 5 - 15 kPa at 1 m depth. Given the very high water content and the sensitive soil fabric, it is challenging to retrieve good quality samples. The sediments are best characterized with in-situ techniques. The relevant stress levels are also significantly smaller than found in conventional foundation engineering. The bearing pressure imposed by pipelines on the seabed is typically in the range 0 – 10 kPa. Such low stress levels are not properly dealt with standard laboratory tests. The merit of Smartpipe is to measure directly the pipe-soil interaction forces in undisturbed soil-conditions and at the appropriate stress level.

Axial pipe-soil response

In soft deep water clay, the pipe-soil axial response is generally undrained, or partially drained, with generation of excess pore pressures at the pipe-soil interface despite the slow rates of movement. In fine-grained sediments, rates as low as a few microns per second may be required to maintain fully drained conditions. The amount of excess pore pressure that is generated depends on many aspects such as the pipe axial velocity, soil stress history, coefficient of consolidation and drainage path length (Hill et al, 2012).

Typical axial pipe-soil responses measured with Smartpipe are illustrated in Figure 4. In these tests, the model pipe was first penetrated into the seabed to an embedment in the range 35% OD to 65% OD, where OD is the pipe outside diameter. Then, a consolidation period of about 4 hours was observed to let the penetration-induced excess pore pressures dissipate. Following the consolidation period, the pipe was displaced axially under constant vertical load.

The axial pipe-soil response in non-linear, with a high initial tangent stiffness progressively reducing until the peak resistance is reached. The breakout peak occurs at an axial displacement of the order of 12 mm (5% OD) and is followed by a residual resistance at larger displacement. The decay to the residual resistance is initially rapid, over about 30 mm (13% OD), followed by a more gentle reduction over a further ~100 mm (45% OD). The residual resistance is observed to be 55 % to 80% of the peak in those tests.

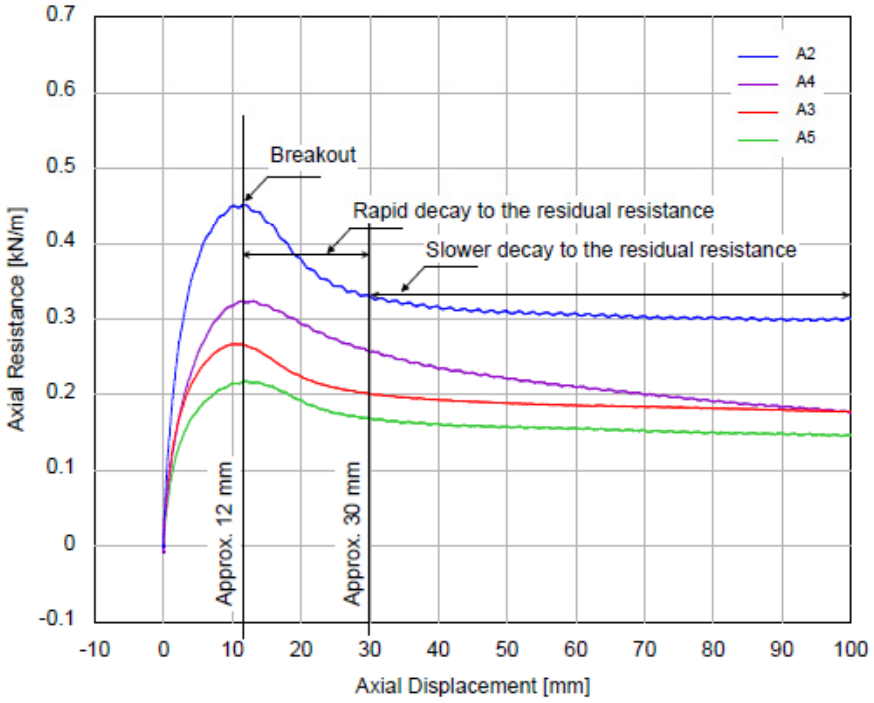

Figure 4 – Typical axial pipe-soil responses.

During the cool-down period, the pipeline is unloaded and the axial displacement is reversed. The unloading response is stiffer and more linear than the loading response with a stiffness similar to the initial tangent stiffness, as shown in Figure 5. The stiffness is about 5 times bigger than the peak secant stiffness in this particular test.

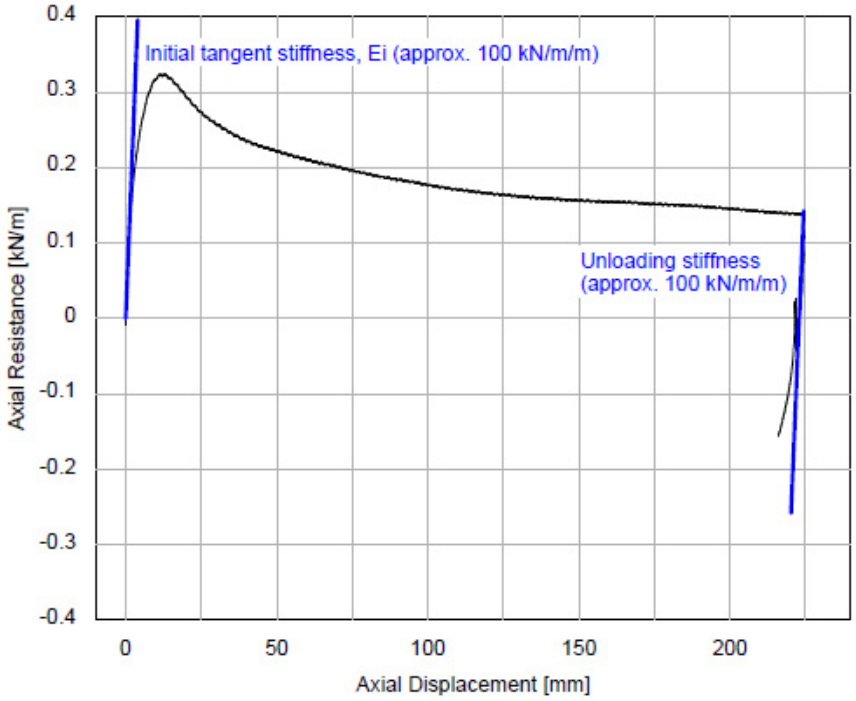

Figure 5 – Axial unloading stiffness.

During reloading cycles, the breakout was also observed to be less pronounced than for the first loading. However, it has been observed that peak recovery is related to time elapsed between cycles and the time between two operating cycles in the field is longer than what has been tested with Smartpipe. The peak mobilisation distance in the reloading cycles is similar to the first loading one.

Smartpipe data have also shown a progressive increase of axial pipe-soil resistance with cycles and consolidation periods. This behaviour has also been observed in interface shear tests and is discussed by White and Cathie (2010). This progressive increase can be explained with critical state soil mechanics concepts. In soft contractile soil, the undrained or partially drained axial pipe-soil resistance is lower than the drained resistance due to the generation of excess pore pressures in the sheared soil around the pipe. During consolidation periods, these excess pore pressures dissipate and the interface zone hardens leading to a rise in axial resistance. When the interface zone has reached the critical state (i.e. shearing under constant volume without generation of excess pore pressures), the axial resistance becomes equal to the fully drained resistance.

There is potentially a great value from a design perspective as it could mean that the low axial resistance associated with undrained shearing of soft contractile soil would be progressively eliminated during the operating life of the pipeline. Therefore, the rate of walking for example would decrease and potentially vanish with operating cycles as the axial resistance converges towards the drained resistance leading to a significantly reduced global pipeline displacement at the end of its design life.

Figure 6 presents an example of Smartpipe results where the residual friction factor f_{aR} (defined as the residual axial resistance F_{aR} divided by the pipe weight and wedging coefficient (White and Randolph, 2007)) is observed to increase from approximately 0.25 to 0.55 in 14 cycles, i.e. an increase of about 0.02 per cycle.

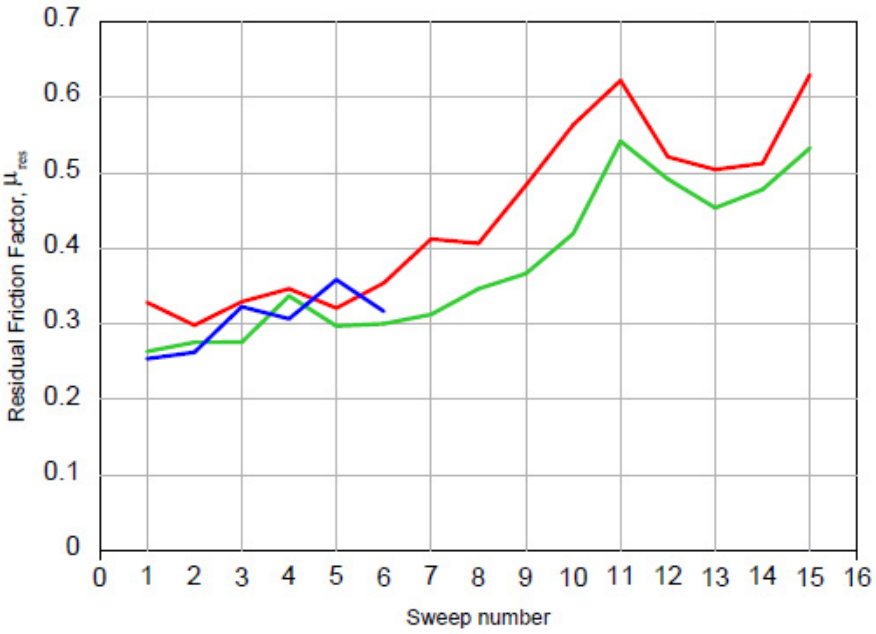

Figure 6 – Evidence of cyclic hardening.

Numerical modeling of pipeline end expansion and walking

In this paper, the influence of pipe soil interaction parameters on the likelihood of pipeline walking is investigated using the SAGE Profile software suite. SAGE Profile has been tailored to assist the pipeline engineer during offshore pipeline design. Using a transient dynamic explicit solver, it can accurately mimic the actual pipeline installation process and simulate the response of the subsea pipe when subjected to hydrodynamic loading and operational conditions (i.e. time-dependent pressure and temperature profiles). A comprehensive overview of the added value SAGE Profile can bring during offshore pipeline design, installation and operation is found in (Van den Abeele, 2012).

As explained in (Carr et al, 2006), pipeline walking can cause cumulative axial displacement of an entire pipeline, which can induce damage at termination units, expansion spools and riser tie-ins. The rate of walking, defined as the accumulated axial displacement per operational cycle, depends not only on the temperature profiles, but also on the magnitude of axial resistance, the mobilization distance and the seabed topography.

The main driving mechanisms for pipeline walking are

- Tension, associated with a steel catenary riser
- Global seabed slope along the pipeline length
- Thermal transients during start-up and shut-down

Although the origin may be different, the walking mechanism for each of these three cases is governed by the effective axial force profile of the pipeline. For a fully restrained, closed-ended pipeline, the effective axial force F_e is the sum of the forces due to axial elongation, internal and external pressure (including end effects) and the temperature gradient ΔT :

$$F_e = \frac{L - L_0}{L_0} EA + (1 - 2\nu)(p_e A_e - p_i A_i) - EA\,\alpha\Delta T \qquad (1)$$

with L_0 the initial length, L the stressed length, A the cross sectional area of the steel, p_e the external pressure acting on the exposed outer surface A_e and p_i the internal surface working on the exposed inner surface A_i. The pipeline steel properties in (01) are the Young's modulus of elasticity E, the Poisson contraction coefficient ν and the coefficient of thermal expansion α respectively.

During cyclic loading of the pipeline, the change in fully constrained force

$$\Delta F = -\Delta p\,(1-2\nu)\,A_i - E\,A\,\alpha\,\Delta T \qquad (2)$$

will dictate the pipeline walking response (Gaillard et al, 2005). In this paper, SAGE Profile is used to evaluate the influence of the pipe soil interaction parameters on the predicted end expansion and walking rate for a pipeline on an inclined seabed.

A straight pipeline of 2 000 meters was modelled on an inclined seabed with a slope θ, subjected to subsequent heating and cooling, similar to the benchmark proposed in Hill et al (2012). To illustrate the fundamental mechanics of pipeline walking, the horizontal soil behaviour was modelled by uncoupled axial and lateral soil springs like shown in Figure 1, i.e. allowing for perfect plasticity. The latter capability is fundamental to accurately model pipeline walking.

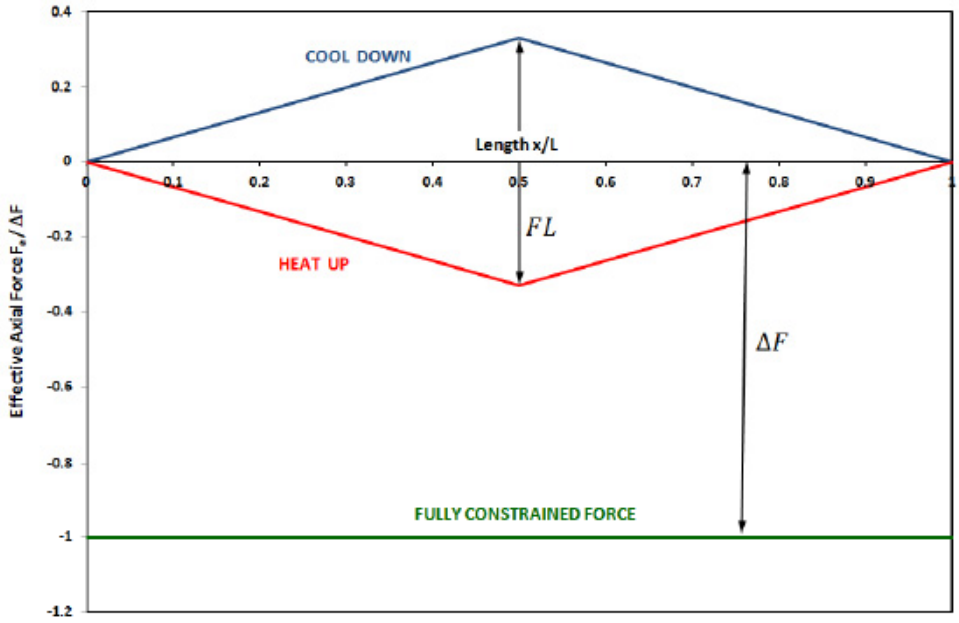

Figure 7 – Force profiles for a fully mobilized 'short' pipeline.

In Figure 7, the general force profiles in fully heated and cool-down conditions are shown for a 'short' pipeline, i.e. the force envelope does not exceed the fully constrained force ΔF. In this situation, the pipeline is fully mobilized and can freely expand and contract around a virtual anchor point.

Generally, the slope of the force profile is defined by the axial friction $f_{ax} = \mu_{ax}\,w_p$, with μ_{ax} the axial friction factor and w_p the submerged pipe weight. On an inclined seabed, the pipe weight promotes expansion in downhill direction, but counteracts the uphill expansion. This is similar to modifying the friction coefficient

$$\mu_\theta = w_p(\mu_{ax}\cos\theta \pm \sin\theta) \qquad (3)$$

which causes an asymmetric force profile envelope (Carr et al, 2006). In Figure 8, the effective axial force profiles predicted by SAGE Profile are shown for a 2 km pipeline on an inclined seabed with slope angle $\theta = 5°$ for heating and cool-down conditions.

For a pipeline that slopes downwards from the inlet, the hot anchor is located closer to the hot end, and the cold anchor closer to the cold end. Hence, the global pipeline displacement is governed by the central section. Such a situation gives rise to a rigid body displacement: the pipe starts to walk down-hill. The walking rate Δ_θ, i.e. the accumulated axial displacement per cycle, can be approximated by (Carr et al, 2006)

$$\Delta_\theta = \frac{\left(\Delta F + w_p L|\sin\theta| - w_p L\,\mu_{ax}\,\cos\theta\right) L \tan\theta}{E\,A\,\mu_{ax}} \qquad (4)$$

The presence of a seabed slope will cause walking for short pipelines with each start-up and shutdown cycle. It is also noted (Carr et al, 2006) that, for a pipeline on an inclined seabed, thermal transients are not required to trigger walking.

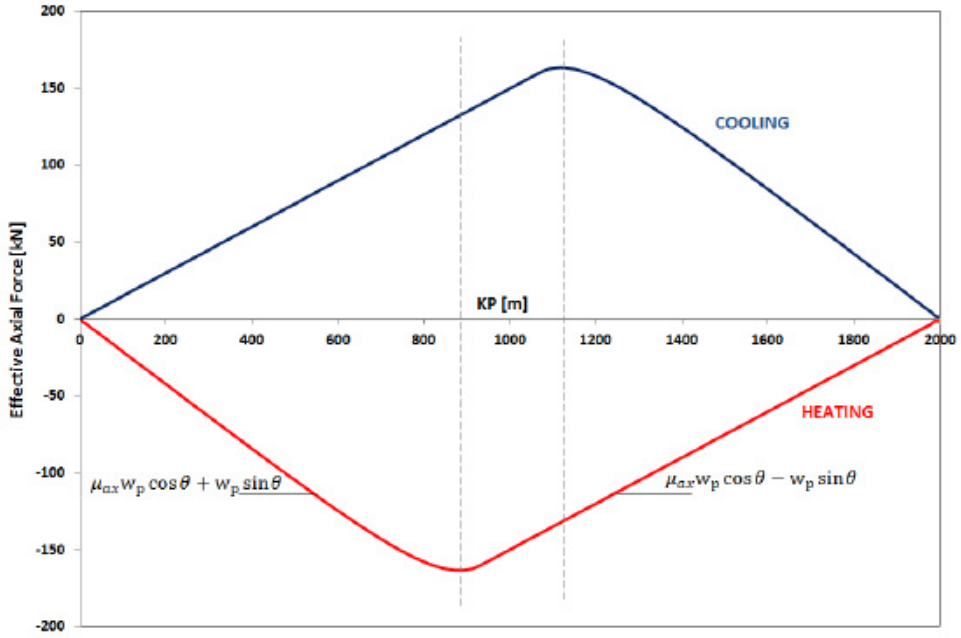

Figure 8 – Effective axial force profiles for a pipeline on a sloping seabed.

In Figure 9, the pipeline response to five subsequent heating and cooling cycles is shown. This figure demonstrates that both pipeline ends move the same amount at the end of each cycle.

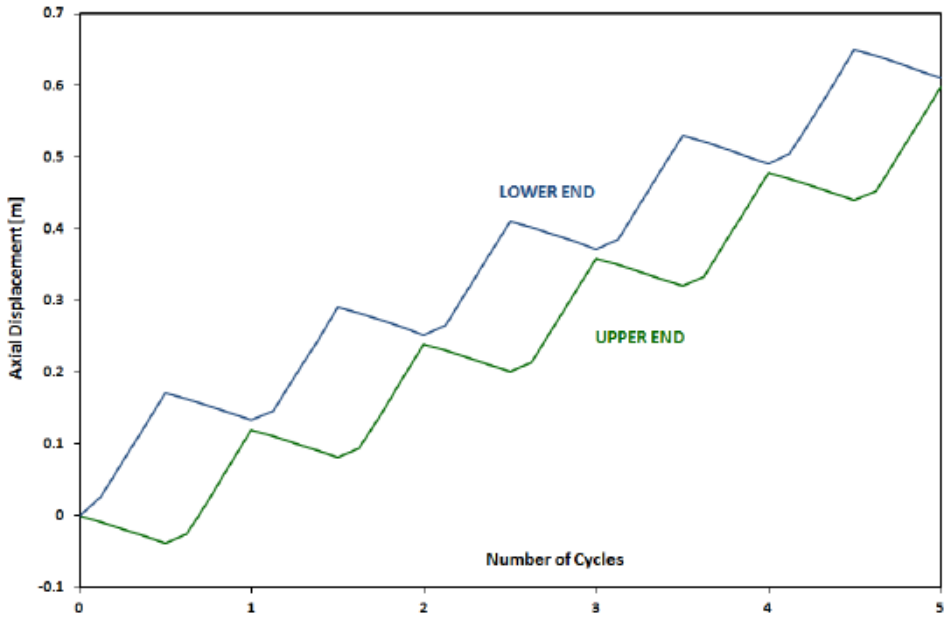

Figure 9 – Pipeline walking over five subsequent cycles.

Thanks to the plastic soil springs with memory components (shown in Figure 1), modelling pipeline walking is feasible with SAGE Profile. In the next sections, the influence of several axial pipe-soil interaction parameters on the predicted walking rate is assessed.

Sensitivity analysis on pipe soil interaction parameters

In this section, the influence of pipe soil interaction parameters on the predicted pipeline end expansion and walking rate is investigated using the SAGE Profile software suite. As a base case, a 2 km pipeline with diameter OD = 225 mm (similar to the SmartPipe tool) and wall thickness 15 mm (corresponding to OD/t = 15) on an inclined seabed is subjected to an operational temperature difference of $\Delta T = 100°$. To confine the sensitivity analysis to the pipe-soil interaction, only a limited temperature gradient (1°C/km) over the pipeline length is assumed.

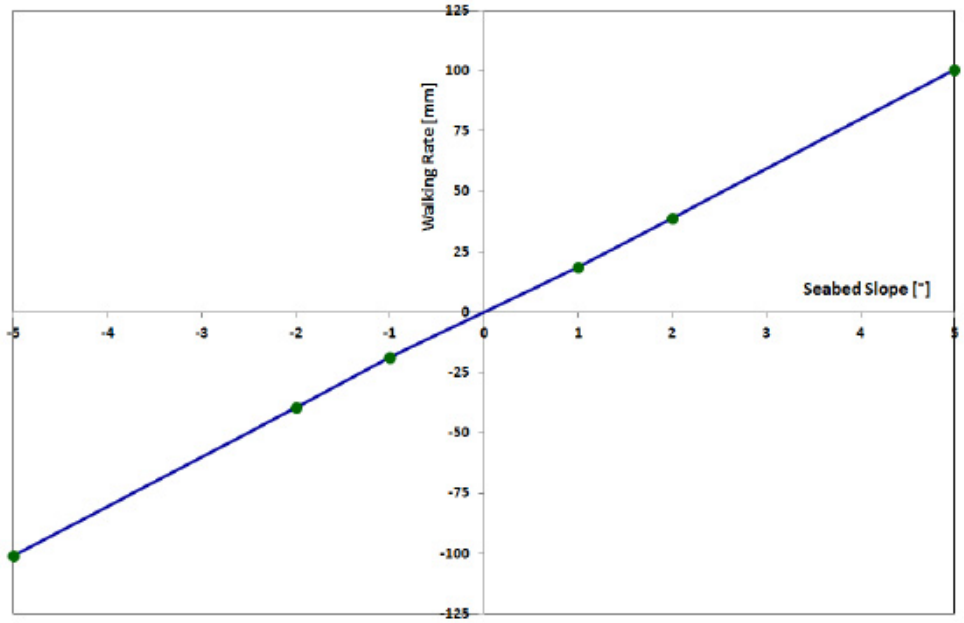

Figure 10 – Influence of slope angle on predicted walking rate.

The influence of the slope angle θ on the predicted walking rate Δ_θ is shown in Figure 10, where a positive angle corresponds to a seabed sloping *down* from the inlet. In the next sections, a seabed with $\theta = +2°$, which induces a walking rate of $\Delta_\theta \approx 40$ mm, is assumed.

Bilinear Axial Soil Springs: friction factor, mobilization distance and unloading stiffness

The axial pipe-soil interaction is commonly captured by a bilinear spring, shown in Figure 1, which can be described in terms of a friction factor μ_{ax} and a mobilization distance D. By default, the unloading stiffness is assumed equal to the loading stiffness defined by $\{\mu_{ax}, D\}$. The influence of the axial friction factor and the corresponding mobilization distance on the thermal expansion of the hot end (during the first operational cycle) is shown in Figure 11.

As can be expected, the thermal expansion reduces with increasing friction factor. Given the fairly high expansion values in this particular case (> 1 m), the influence of mobilization distance is limited. For increasing mobilization distance, the expansion is lower, because it takes somewhat longer before the full axial resistance is fully mobilized.

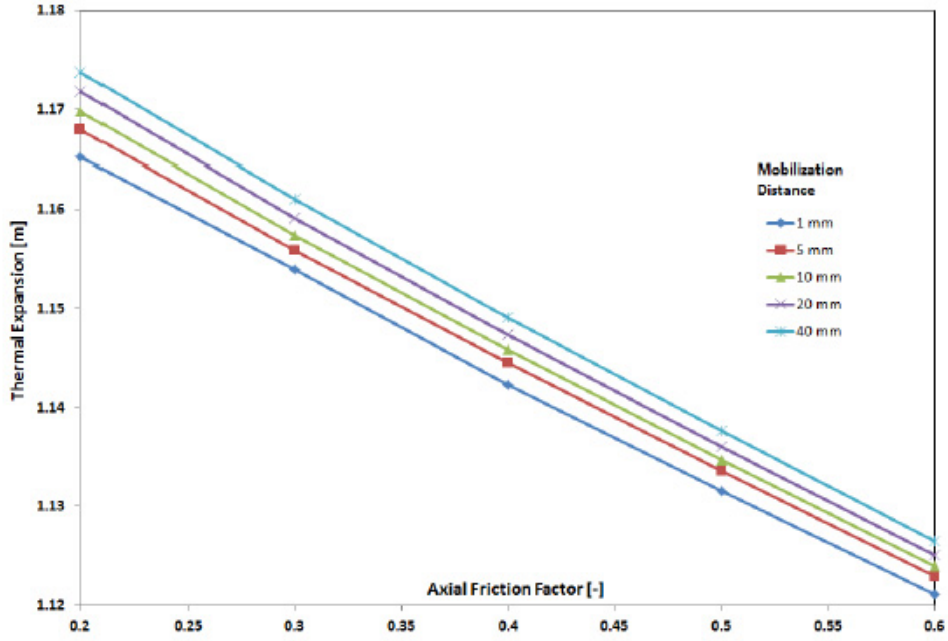

Figure 11 – Influence of friction factor and mobilization distance on thermal expansion.

The influence of friction factor and mobilization distance on the predicted walking rate is shown in Figure 12. Unsurprisingly, the walking rate decreases with increasing axial friction factor. For the mobilization distance, the trend is reversed: the walking rate is lower for higher values of the mobilization distance. This can be attributed by the unloading stiffness: the first heat-up cycle induces a high thermal expansion (> 1 m), where the influence of the mobilization distance is not significant (see Figure 12). However, the mobilization distance also dictates the slope of the unloading curve. For high mobilization distances, lower permanent soil deformation is predicted, indeed resulting in a lower value for the walking rate. Finally, the influence of the mobilisation distance on the predicted waking rate increases with increasing axial friction factor.

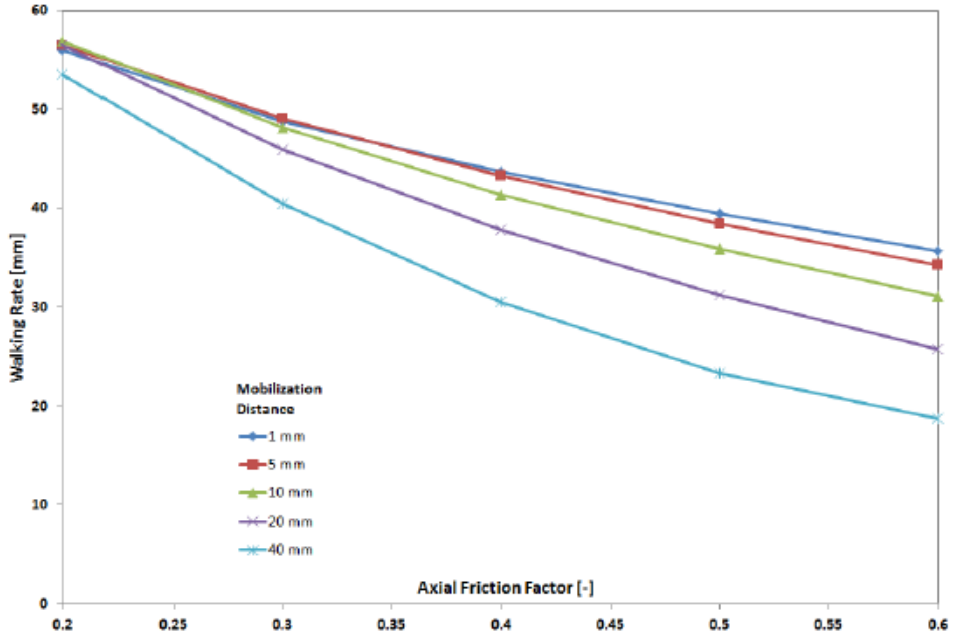

Figure 12 – Influence of friction factor and mobilization distance on walking rate.

The influence of the unloading stiffness is further elaborated in Figure 13, where the walking rate is shown for a fixed friction factor $\mu_{ax} = 0.5$, as the unloading stiffness is progressively swept from 1.0 to 10 times the initial loading stiffness, determined by $\{\mu_{ax}, D\}$.

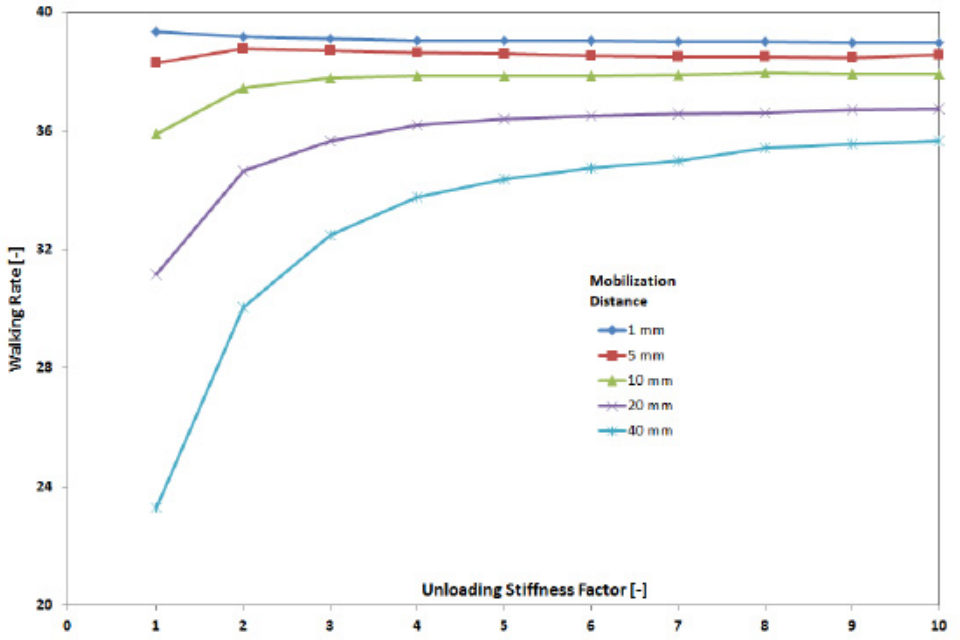

Figure 13 – Influence of unloading stiffness on walking rate.

For low mobilization distances, the walking rate is not sensitive to the unloading stiffness, as the unloading is almost immediate. For higher values of mobilization distance, the unloading stiffness governs the amount of permanent soil deformation and hence has a more pronounced influence on the walking rate. This observation adds weight to the importance of correctly calibrating the unloading stiffness of the axial soil spring: underestimating the unloading stiffness may give an erroneous prediction of the walking rate, and hence a non-conservative design!

Trilinear soil springs: influence of peak to residual friction factor ratio

SAGE Profile allows introducing more enhanced pipe-soil interaction behaviour through its external pipe soil interaction module (XSPIM). In this paper, we have used the XSPIM library to model the axial soil spring as a tri-linear curve, which enables distinguishing between the peak friction factor μ_P, which is reached at a 'mobilization' distance D_P, and the residual friction factor μ_R, which is reached at a 'mobilization' distance D_R. In addition, the XSPIM model allows selecting an unloading stiffness and re-loading stiffness which is different than the original first-loading stiffness, defined by $\{\mu_P, D_P\}$. The tri-linear axial soil spring is schematically shown in Figure 14.

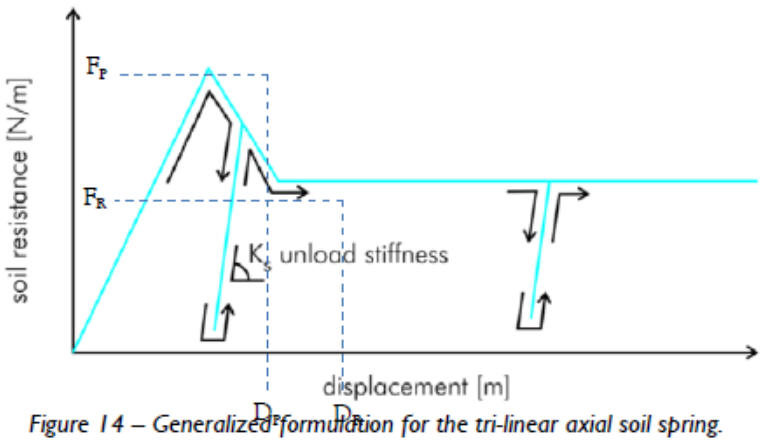

Figure 14 – Generalized formulation for the tri-linear axial soil spring.

For this analysis, the unloading and reloading stiffness is assumed to be the same as the initial first load stiffness, determined by $\{\mu_p, D_p\}$, and the residual friction factor is chosen to be $\mu_R = 0.3$. A sensitivity analysis is performed by sweeping the value for μ_p from $1.0\,\mu_R$ to $2.0\,\mu_R$. The (peak) mobilization distances of the previous sections are investigated, assuming a fixed ratio D_R/D_p= 3.0, as suggested by Smartpipe results.

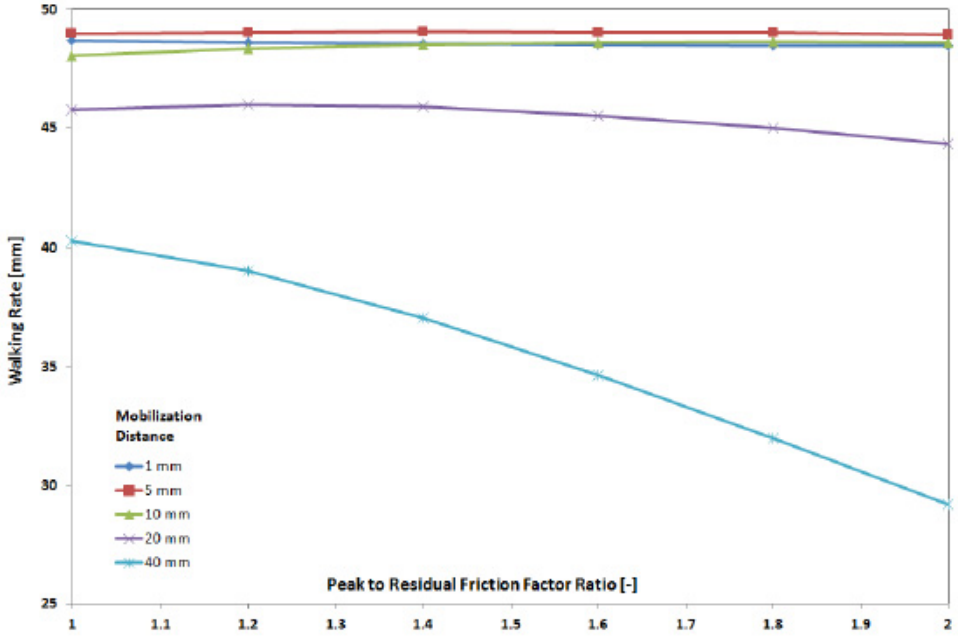

Figure 15 – Walking rate for different values of peak-to-residual friction factor.

The influence of the peak-to-residual friction factor ration μ_p/μ_R on the predicted walking rate is shown on Figure 15. For (very) small values of mobilization distance, the presence of the peak does not influence the walking rate. For larger values of mobilization distance, the walking rate clearly decreases with increasing values for μ_p/μ_R, thanks to the presence of the peak. Therefore, in some cases, the modelling of the peak-residual response may be beneficial for pipeline design.

Influence of cyclic hardening

Smartpipe data have shown a progressive increase of axial pipe-soil resistance with cycles and consolidation periods, as demonstrated in Figure 6. There is potentially a great value from a design perspective as it could mean that the low axial resistance associated with undrained shearing of soft contractile soil would be progressively eliminated during the operating life of the pipeline.

To investigate the influence of cyclic hardening on the walking rate, we have simulated ten consecutive heating and cooling cycles. The axial pipe-soil interaction was modelled with a bilinear spring with a very low mobilisation distance (1 mm), where the axial friction factor progressively increases from $\mu_{ax} = 0.3$ to $\mu_{ax} = 0.5$, i.e. an increase of $\Delta\mu_{ax} = 0.02$ for each operational cycle.

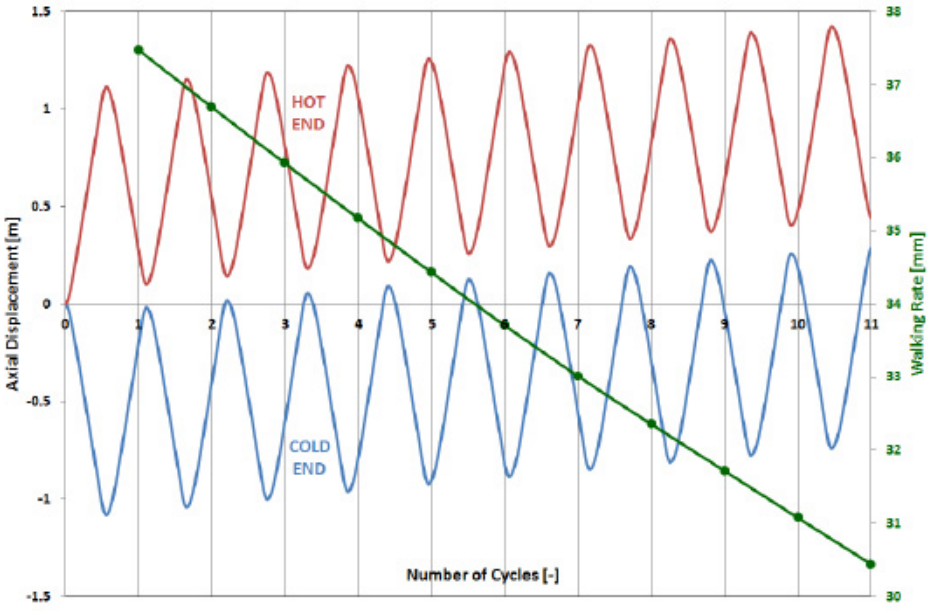

Figure 16 – Influence of cyclic hardening on pipeline walking.

The pipeline response, shown in Figure 16, clearly reveals a decreasing walking rate with the increasing axial resistance associated with cyclic hardening. This reducing walking rate can make a significant difference to the total axial displacement accumulated over the design life of the pipeline.

Conclusions

In this paper, parametric FE analyses were presented using the SAGE Profile software suite for offshore pipeline analysis. The results indicate that the powerful pipe-soil interaction library of SAGE Profile is capable of accurately capturing the phenomenon of axial walking. More sophisticated axial pipe-soil responses, derived from the SMARTPIPE measurements, were implemented to assess the impact on the predicted end expansion and walking rate. The axial pipe-soil interaction was captured by a tri-linear soil spring, and the effects of mobilization distance, peak friction factor and residual friction factor were evaluated by performing sensitivity analyses. Moreover, the trilinear soil spring in SAGE Profile allows distinguishing between the initial (first loading) stiffness, the unloading stiffness and the reloading stiffness.

The parametric analyses have shown the following for the particular case analysed in this paper:

- The predicted walking rate decreases with increasing mobilisation distance and the influence of mobilisation distance increases with increasing axial friction factors.
- The unloading/reloading stiffness governs the predicted walking rate and should be selected with care. Smartpipe results indicate an unloading stiffness that is about five times the first loading secant stiffness.
- In some cases, the modelling of the peak-residual axial response may be beneficial for pipeline design as it reduces the predicted walking rate.
- Cyclic hardening gives rise to a decreasing walking rate, which can lead to a significantly reduced total pipeline axial displacement over the operating life of the pipeline. This is potentially of great value from a design perspective.

References

1. Ballard J.C, Jewell R., de Brier C. and Stassen K. (2013). Observations of pipe soil response from in-situ measurements. Proc. of Offshore Technology Conference, Houston, Texas, USA, OTC paper 24154.
2. Bruton D. A. S., White D. J., Carr M. C. and Cheuk C. Y. (2008). Pipe-soil interaction during lateral buckling and pipeline walking: The SAFEBUCK JIP. Proc. of Offshore Technology Conference, Houston, Texas, USA, OTC Paper 19589.
3. Bruton D.A. S., F. Sinclair and M. Carr (2010). Lessons learned from observing walking of pipelines with lateral buckles, including new driving mechanisms and updated analysis models. Proc. of Offshore Technology Conference, Houston, Texas, USA, OTC paper 20750.
4. Carneiro D. and Murphy D. (2011), Simple Numerical Models for Pipeline Walking accounting for Mitigation and Complex Soil Response, Proceedings of the 30th International Conference on Ocean, Offshore and Arctic Engineering, OMAE2011-49780
5. Carr M., Sinclair F. and Bruton D. (2006). Pipeline walking – Understanding the field layout challenges, and analytical solutions developed for the Safebuck JIP. Proc of Offshore Technology Conference, Houston, Texas, USA, paper OTC 17945.
6. Denis R. and de Brier C. (2010). Deep water tool for in-situ pipe-soil interaction measurement: recent developments and system improvement. Proc. of Offshore Technology Conference, Houston, Texas, USA, OTC paper 20630.
7. Gaillard C.S. and Williams K. (2005), Pipeline Walking, Proceedings of the Offshore Pipeline Technology Conference, OPT
8. Hill A.J. and Jacob H. (2008). In-situ measurement of pipe-soil interaction in deep water. Proc. of Offshore Technology Conference, Houston, Texas, USA, OTC Paper 19528.
9. Hill A., White D.J., Bruton D.A.S., Langford T., Meyer V., Jewell R. & Ballard J-C. (2012). New datasets and improved framework for axial pipe-soil resistance. Proc. Int. Conf. on Offshore Site Investigation and Geotechnics. SUT, London.
10. Looijens P. and Jacob H. (2008). Development of a deepwater tool for in-situ pipe-soil interaction measurement and benefits in pipeline analysis. Proc. 31st Offshore Pipeline Technology Conference, Amsterdam, The Netherlands.
11. Van den Abeele F. and Denis R. (2012), Numerical Modelling and Analysis for Offshore Pipeline Design, Installation and Operation, Journal of Pipeline Engineering, Q4, pp. 273-286
12. White D.J. and Randolph M.F. (2007). Seabed characterization and models for pipe-soil interaction. Int. Journal of Offshore & Polar Engng. 17(3):193-204.
13. White D.J., Hill A.J., Westgate Z.J. and Ballard J.C. (2010). Observations of pipe-soil response from the first deep water deployment of the Smartpipe. 2nd International Symposium on Frontiers in Offshore Geotechnics (ISFOG), Perth, Western Australia.
14. White D.J. and Cathie D.N. (2010). Geotechnics for subsea pipelines. Proc. 2nd Int. Symp. on Frontiers in Offshore Geotechnics, Perth, Western Australia.
15. Witgens J.F., Falepin H. and Stephan L. (2006), New Generation Pipeline Analysis Software, Offshore Pipeline Technology, OPT